MMSE-Based MIMO Receiver for Cooperative Downlink NOMA in LEO Satellite Networks

Jeong Seon Yeom, Yujin Lee, and Bang Chul Jung
Department of Electronics Engineering
Chungnam National University
Daejeon, South Korea
Email: jsyeom@cnu.ac.kr, leeuj@o.cnu.ac.kr, bcjung@cnu.ac.kr

Abstract—We propose a novel minimum mean square error (MMSE)-based receiver with multiple antennas for downlink cooperative non-orthogonal multiple access (NOMA) systems in low earth orbit (LEO) satellite networks. In this paper, we focus on a common user equipment (UE) that exists in a cell cross-region serviced by two adjacent satellites. With the proposed technique, the common UE utilizes the advantage of multiple receiving antennas when receiving the NOMA signal containing its own signal through orthogonal frequencies from both two satellites. Through computer simulations, we show that the proposed MMSE-based NOMA receiver outperforms the conventional selection combining-based receiver in terms of bit-error rate performance.

Index Terms—6G, low earth orbit (LEO) satellite communication, non-orthogonal multiple access (NOMA), multiple antennas, bit-error rate (BER), minimum mean square error (MMSE).

Fig. 1. System model of LEO satellite network including UEs present in a cell cross-region.

I. INTRODUCTION

Recently, satellite communication is one of the most promising industries, and a lot of research is being conducted in academia. In particular, low-earth orbit (LEO) satellite communication systems are attracting much attention because they can provide about $10 \sim 20$ times the satellite delay compared to geostationary orbit satellite communication systems. The advantage of the satellite communication system for 6th generation (6G) mobile communication system is that it can support the global coverage and can also improve mobility performance [1], [2]. In this paper, we deal with a direct connection of user equipment (UE)-to-LEO satellite without a ground station platform to improve UE accessibility [3].

In the last decade, non-orthogonal multiple access (NOMA) technique has been one of the most studied techniques to improve spectral efficiency and latency in mobile wireless communications [4], [5]. In power domain-NOMA system, a receiver simultaneously receives two or more signals on the same frequency and same code and decodes desired information from the superimposed received signal by using successive interference cancellation (SIC) or joint maximum likelihood (JML) detectors [6], [7].

There are several literature in which NOMA technique is applied to a forward terminal link (called as downlink in cellular network) of LEO satellite communication. LEO satellite forms multiple beams serving different regions and transmits a independent NOMA signal for each beam [8], [9]. In [8], LEO satellite equipped with a uniform planar array antenna precodes a transmit NOMA signal to maximize the sum-rate performance. In [9], LEO sa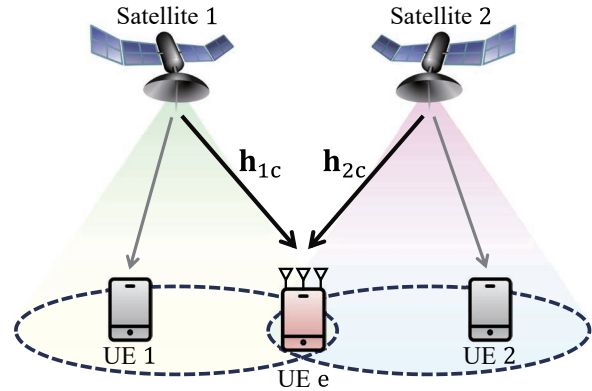tellite forms multiple beams by using an array fed reflector antenna. Considering a power limited LEO satellite system, authors proposed a beamforming algorithm for minimizing the total power consumption. In order to improve the channel quality of direction link, reconfigurable intelligent surface (RIS) was considered [10]. The use of RIS is one of the solutions that can improve energy efficiency and frequency efficiency at the same time in LEO satellite communication systems. In [11], the authors consider two adjacent satellites simultaneously servicing one common UE using NOMA technique. The common UE decodes its own signal from a signal with a higher signal-to-noise ratio (SNR) between two superimposed signals via orthogonal frequencies.

In most of the literature, LEO satellites with available power limits sacrifice the computational burden, and a UE is equipped with with a single antenna. We extend the number of antenna of the common UE to N in the system model of [11] and consider a received minimum mean square error (MMSE) beamforming based receiver to improve a bit-error rate (BER) performance. And, this receiver can provide lower computational complex than the conventional detection schemes. Through computer simulation results, it is shown that the proposed MMSE-based NOMA receiver for common UE outperforms the selective combining (SC) scheme applied in [11] in terms of the BER performance.

II. SYSTEM MODEL

We consider LEO satellite system consisting of two adjacent satellites and three UEs (UE 1, UE 2, and UE e called as the common UE) over the forward terminal link. We assume that

this satellite system is based on earth fixed cell and direct connection system, and adjacent earth fixed cells are assigned orthogonal frequency bands. UE 1 and UE 2 are located in the center of the service cells of satellite 1 and 2, respectively, while UE e which is equipped with N antennas is located at the intersection of the two cells as shown in Fig. 1.

In order to improve the spectral efficiency, we apply the NOMA technique, and then satellite $k \in \{1, 2\}$ transmits a signal in which the signal of UE k and the signal UE e are overlapped via k-th orthogonal frequency band. In this paper, we focus on a reception scheme of the UE c because UE k can adapt a conventional detector such as the SIC or JML detectors. Therefore, a received signal column vector, $\begin{bmatrix} \mathbf{y}_1 & \mathbf{y}_2 \end{bmatrix}^T \in \mathbb{C}^{2N}$, of the UE e is given as follows:

$$
\begin{aligned}
\begin{bmatrix} \mathbf{y}_1 \\ \mathbf{y}_2 \end{bmatrix} &= \begin{bmatrix} \sqrt{P_1 L_{1e}} \mathbf{h}_{1e} \left(\sqrt{\alpha_1} x_e + \sqrt{1-\alpha_1} x_1 \right) \\ \sqrt{P_2 L_{2e}} \mathbf{h}_{2e} \left(\sqrt{\alpha_2} x_e + \sqrt{1-\alpha_2} x_2 \right) \end{bmatrix} + \begin{bmatrix} \mathbf{n}_1 \\ \mathbf{n}_2 \end{bmatrix} \\
&= \underbrace{\begin{bmatrix} \sqrt{P_1 L_{1e} \alpha_1} \mathbf{h}_{1e} \\ \sqrt{P_2 L_{2e} \alpha_2} \mathbf{h}_{2e} \end{bmatrix}}_{\triangleq \mathbf{g}_e, \text{ Desired signal channel}} x_e + \begin{bmatrix} \mathbf{n}_1 \\ \mathbf{n}_2 \end{bmatrix} \\
&\quad + \underbrace{\begin{bmatrix} \sqrt{P_1 L_{1e}(1-\alpha_1)} \mathbf{h}_{1e} & \mathbf{0}_{N \times 1} \\ \mathbf{0}_{N \times 1} & \sqrt{P_2 L_{2e}(1-\alpha_2)} \mathbf{h}_{2e} \end{bmatrix}}_{\triangleq \mathbf{G}_I, \text{ Interference channel}} \begin{bmatrix} x_1 \\ x_2 \end{bmatrix}, \quad (1)
\end{aligned}
$$

where $\mathbf{y}_k$ $(k \in \{1, 2\})$ denotes the received signal vector from the k-th satellite to the UE e via k-th frequency band, and x_u $(u \in \{1, 2, e\})$ denotes a signal of UE u. And, P_k and α_k denote a transmit power of the satellite k and a power allocation factor at the satellite k, respectively. The variable L_{ke} is a link gain including a total path loss, PL_{ke}, and a radio frequency (RF) gain, G_{ke}, between a transmitter of the satellite k and a receiver of UE e, i.e., $L_{ke} = G_{ke} \times PL_{ke}^{-1}$. The fading channel column vector, $\mathbf{h}_{ke} \in \mathbb{C}^N$, from the satellite k to the UE e is assumed to follow shadowed Rician distribution. The path loss model and fading channel model are described in detail in the following subsection. Additive white Gaussian noise at the UE e over k-th frequency band is denoted as $\mathbf{n}_k$, each element of which is i.i.d. complex Gaussian random variable with zero mean and N_0 variance.

A. Channel Model from LEO Satellite to Terrestrial UE

In this subsection, we describe in detail the channel model that should be considered in the forward terminal link of LEO satellite communication. For notational simplicity, we sometimes omit subscripts of above mathematical symbols.

The channel model is divided into the link path loss part, the small scale channel part, and the RF gain part. First, as described in [12, Ch. 6.6.2], the path loss, L_{ke}, including a large scale channel in dB is composed as follows:

$$PL = PL_b + PL_g + PL_s + PL_e, \quad (2)$$

where PL_b, PL_g, PL_s, and PL_e denote the basic path loss, the attenuation due to atmospheric gasses, the attenuation due to either ionospheric or tropospheric scintillation, and building entry loss, respectively.

Specifically, the basic path loss in dB is modeled as follows:

$$PL_b = FSPL(d, f_c) + SF + CL(\theta_E, f_c), \quad (3)$$

where $FSPL$ and CL denote the free space path loss (FSPL) and clutter loss, respectively, and SF is shadow fading following Gaussian distribution, i.e., $SF \sim \mathcal{N}\left(0, \sigma_{SF}^2\right)$. The FSPL is given as follows:

$$FSPL(d, f_c) = 32.45 + 20 \log_{10}(f_c) + 20 \log_{10}(d). \quad (4)$$

The value of σ_{SF}^2 and CL are given as [12, Tab. 6.6.2-1 to 6.6.2-3]. In (3), the arguments d, f_c, and θ_E denote a slant distance in meter, carrier frequency in Ghz, and elevation angle from the UE to the satellite relative to the horizon, respectively. The slant distance can be determined by a satellite altitude h_0 and the elevation angle as $d = \sqrt{R_E^2 \sin^2(\theta_E) + h_0^2 + 2h_0 R_E} - R_E \sin(\theta_E)$ where R_E denotes the earth's radius, i.e., $R_E = 6,371$ km.

The attenuation by atmospheric gasses depends mainly on frequency, elevation angle, altitude above sea level, and water vapour density and is given as follows:

$$PL_g = A_{\text{zenith}}(f_c) / \sin(\theta_E), \quad (5)$$

where A_{zenith} denotes a zenith attenuation and is provided for frequencies between 1 and 1000 GHz in [13, Fig. 4].

The scintillation loss PL_s is caused by ionospheric or tropospheric propagation. Generally, ionospheric and tropospheric propagation shall only be considered for frequencies below 6 Ghz and above 6 Ghz, respectively.

The building entry loss PL_e for a indoor UE is the additional loss between the UE and adjacent outdoor path. It is determined by a thermal efficiency and traditional [13].

In addition, rain and cloud attenuation should be also considered for frequencies above 6 Ghz. However, as a baseline we assume clear sky conditions, and then this attenuation is negligible in this paper.

Second, the small scale channel is generally modeled as shadowed Rician fading channel including both line-of-sight (LoS) and non-LoS (NLoS) components. The shadowed Rician fading channel coefficient is given as follows:

$$[h_{ke}]_n = \sqrt{\frac{\kappa}{\kappa+1}} h_{\text{LoS},k} + \sqrt{\frac{1}{\kappa+1}} h_{\text{NLoS},k}, \quad (6)$$

where κ denotes a Rician factor, and $h_{\text{LoS},k}$ and $h_{\text{NLoS},k}$ denote a LoS channel coefficient and a NLoS channel coefficient, respectively. The two complex-valued channel coefficients follow the following distributions.

$$
\begin{aligned}
|h_{\text{LoS},k}| &\sim \text{Nakagami}(m, \Omega), & \angle h_{\text{LoS},k} &\sim \text{Unif}[0, 2\pi), \\
|h_{\text{NLoS},k}| &\sim \text{Rayleigh}(\sigma_R), & \angle h_{\text{NLoS},k} &\sim \text{Unif}[0, 2\pi),
\end{aligned}
$$

where m and Ω denote a shape parameter and a parameter controlling spread, respectively, and σ is related to an average value of magnitude of NLoS channel coefficient.

Third, RF gain, G_{ke}, is given by the product of an antenna gain of UE e, G_e, an maximum antenna gain of the LEO satellite, $G_{k,\max}$, and a beam gain, $b_{ke}(\phi_{ke})$, where ϕ_{ke} denotes an angle between the beam center and the UE e with respect to LEO satellite k and b_{ke} for a tapered aperture antenna is approximately modeled by [9]–[11]

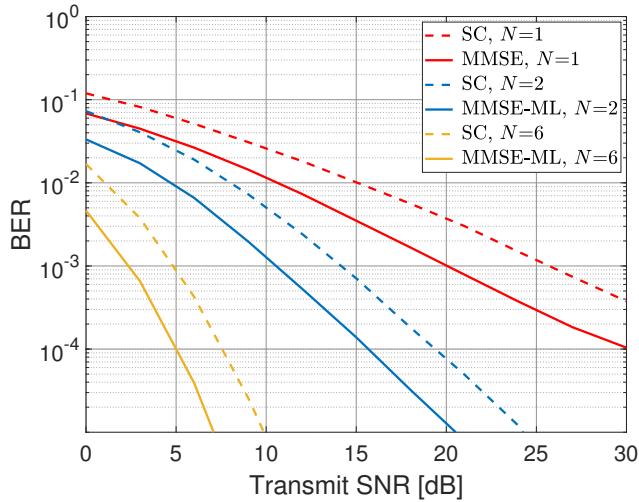$$b_{ke}(\phi_{ke}) = \left(\frac{J_1(u_k)}{2u_k} + 36 \frac{J_3(u_k)}{u_k^3} \right)^2, \quad (7)$$

Fig. 2. BER performance of proposed MMSE-based NOMA receiver for varying the transmit SNR when $N \in \{1, 2, 3\}$.

where J_p denotes the Bessel function of the first kind and order p and $u_k \triangleq 2.07123 \times \sin(\phi_{ke}) / \sin(\phi_{3dB})$. The angle ϕ_{3dB} denotes an antenna 3 dB (half power) beamwidth.

III. PROPOSED MMSE-BASED NOMA RECEIVER

The received MMSE beamforming is known as a beamforming technique that maximizes the signal-to-interference-plus-noise ratio (SINR) by whitening the interference channel. In this system model, the received MMSE beamforming vector, $\mathbf{w}$, is given by

$$\mathbf{w} = \frac{\mathbf{g}_e^H \left(\mathbf{G}_I \mathbf{G}_I^H + N_0 \mathbf{I}_{2N} \right)^{-1}}{\left\| \mathbf{g}_e^H \left(\mathbf{G}_I \mathbf{G}_I^H + N_0 \mathbf{I}_{2N} \right)^{-1} \right\|}. \tag{8}$$

Therefore, a effective received signal is given by

$$\bar{y} = \mathbf{w}\mathbf{y} = \mathbf{w}\mathbf{g}_e x_e + \mathbf{w}\mathbf{G}_I \begin{bmatrix} x_1 & x_2 \end{bmatrix}^T + \mathbf{w} \begin{bmatrix} \mathbf{n}_1 & \mathbf{n}_2 \end{bmatrix}^T, \tag{9}$$

and then the receiver detects bit information through the maximum likelihood method as follows:

$$\hat{x}_e = \underset{s_e \in \mathcal{X}}{\arg \min} \left\| \bar{y} - \mathbf{w}\mathbf{g}_e s_e \right\|^2, \tag{10}$$

where $\mathcal{X}$ denotes a set of candidates of modulated symbol x_e.

IV. SIMULATION RESULTS

The simulation parameters are given as $f_c = 28$ Ghz, $h_0 = 780$ km, $\theta_E = 60°$, i.e., $d = 884.85$ km, $\sigma_{SF} = 4$, $A_{zenith} = 0.22$, $PL_s = 0.13$ dB (worst case), $PL_e = 0$ dB, $G_e = 1$ dBi, $G_{k,max} = 17$ dBi, $\phi_{3dB} = 28°$, $\sigma_R = 1$, $\kappa = 1$, $m = 1$, $\Omega = 1$, and $(\alpha_1, \alpha_2) = (0.7, 0.6)$. We assume the LoS channel between LEO satellite and UE e, and then $CL = 0$.

Fig. 2 shows the BER performance of proposed MMSE-based NOMA receiver for varying the transmit SNR when $N \in \{1, 2, 6\}$, $P_1 = P_2$, and the signal is modulated by quadrature phase shift keying. The SC scheme [11] is considered as the baseline scheme, and the maximum likelihood detection technique is applied to signal detection of UE e in multiple antenna cases. The proposed MMSE-based NOMA receiver outperforms the existing SC scheme in the entire SNR

region. As the number of antennas decreases. the dimension of the signal also decreases, so the performance of maximum likelihood detection applied to the SC scheme suffers, resulting in a large performance difference from the proposed receiver.

V. CONCLUSION

In this paper, we proposed a minimum mean square error (MMSE)-based non-orthogonal multiple access (NOMA) receiver in a low earth orbit (LEO) satellite communication applied with NOMA technique. A common user equipment (UE) in a cell cross-region of two adjacent LEO satellites receives different NOMA signals from two satellites and performs the linear combining for maximizing signal-to-interference-plus-noise ratio rather than a traditional NOMA detection. Compared to existing selection combining scheme considered as the baseline scheme, it was confirmed that the proposed NOMA receiver provides superior bit-error rate performance.

REFERENCES

[1] X. Lin, S. Cioni, G. Charbit, N. Chuberre, S. Hellsten, and J.-F. Boutillon, "On the path to 6G: Embracing the next wave of low earth orbit satellite access," *IEEE Commun. Mag.*, vol. 59, no. 12, pp. 36–42, Dec. 2021.

[2] Z. Xiao, J. Yang, T. Mao, C. Xu, R. Zhang, Z. Han, and X.-G. Xia, "LEO satellite access network (LEO-SAN) towards 6G: Challenges and approaches," *IEEE Wireless Commun.*, Dec. 2022 (early access).

[3] J. A. Fraire, O. Iova, and F. Valois, "Space-terrestrial integrated internet of things: Challenges and opportunities," *IEEE Commun. Mag.*, vol. 60, no. 12, pp. 64–70, Sept. 2022.

[4] S. M. R. Islam, N. Avazov, O. A. Dobre, and K.-S. Kwak, "Power-domain non-orthogonal multiple access (NOMA) in 5G systems: Potentials and challenges," *IEEE Commun. Surveys Tuts.*, vol. 19, no. 2, pp. 721–742, 2nd Quart. 2017.

[5] Y.-K. Bae, J. S. Yeom, and B. C. Jung, "Performance analysis of uplink index-modulated NOMA for 6G wireless communications," *IEEE Wireless Commun. Lett.*, vol. 12, no. 8, pp. 1404–1408, Aug. 2023.

[6] J. S. Yeom, H. S. Jang, K. S. Ko, and B. C. Jung, "BER performance of uplink NOMA with joint maximum-likelihood detector," *IEEE Trans. Veh. Technol.*, vol. 68, no. 10, pp. 10 295–10 300, Oct. 2019.

[7] Y.-B. Kim, K. Yamazaki, and B. C. Jung, "Virtual full-duplex cooperative NOMA: Relay selection and interference cancellation," *IEEE Trans. Wireless Commun.*, vol. 18, no. 12, pp. 5882–5893, Dec. 2019.

[8] Z. Gao, A. Liu, C. Han, and X. Liang, "Sum rate maximization of massive MIMO NOMA in LEO satellite communication system," *IEEE Wireless Commun. Lett.*, vol. 10, no. 8, pp. 1667–1671, Aug. 2021.

[9] J. Chu, X. Chen, C. Zhong, and Z. Zhang, "Robust design for NOMA-based multibeam LEO satellite internet of things," *IEEE Internet Things J.*, vol. 8, no. 3, pp. 1959–1970, Feb. 2021.

[10] W. U. Khan, E. Lagunas, A. Mahmood, S. Chatzinotas, and B. Ottersten, "Energy-efficient RIS-enabled NOMA communication for 6G LEO satellite networks," *arXiv*:2303.05588, Mar. 2023.

[11] B. M. Elhalawany, C. Gamal, A. Elsayed, M. M. Elsherbini, M. M. Fouda, and N. Ali, "Outage analysis of coordinated NOMA transmission for LEO satellite constellations," *IEEE Open J. Commun. Soc.*, vol. 3, pp. 2195–2202, Nov. 2022.

[12] *Study on New Radio (NR) to support non-terrestrial networks (Release 15)*, 3GPP TR 38.811 V15.4.0, Sept. 2020.

[13] *Attenuation by atmospheric gases and related effects*, ITU Recommendation ITU-R P.676-12, Aug. 2019.